This article was downloaded by: [Renmin University of China]
On: 13 October 2013, At: 10:51
Publisher: Taylor & Francis
Informa Ltd Registered in England and Wales Registered Number: 1072954 Registered office: Mortimer House, 37-41 Mortimer Street, London W1T 3JH, UK

Journal of Coordination Chemistry
Publication details, including instructions for authors and subscription information:
http://www.tandfonline.com/loi/gcoo20

Two copper(II) metal-organic networks derived from bis-pyridyl-bis-amide ligands and aromatic polycarboxylates: a 2-D layered structure and a 4-connected trinodal 3-D topology

Hongyan Lin [a], Peng Liu [a], Juwen Zhang [a], Xiuli Wang [a] & Guocheng Liu [a]

[a] Department of Chemistry, Liaoning Province Silicon Materials Engineering Technology Research Centre, Bohai University, Jinzhou, P.R. China

Accepted author version posted online: 16 Jan 2013.Published online: 28 Feb 2013.

To cite this article: Hongyan Lin, Peng Liu, Juwen Zhang, Xiuli Wang & Guocheng Liu (2013) Two copper(II) metal-organic networks derived from bis-pyridyl-bis-amide ligands and aromatic polycarboxylates: a 2-D layered structure and a 4-connected trinodal 3-D topology, Journal of Coordination Chemistry, 66:4, 612-623, DOI: 10.1080/00958972.2013.766333

To link to this article: http://dx.doi.org/10.1080/00958972.2013.766333

PLEASE SCROLL DOWN FOR ARTICLE

Taylor & Francis makes every effort to ensure the accuracy of all the information (the “Content”) contained in the publications on our platform. However, Taylor & Francis, our agents, and our licensors make no representations or warranties whatsoever as to the accuracy, completeness, or suitability for any purpose of the Content. Any opinions and views expressed in this publication are the opinions and views of the authors, and are not the views of or endorsed by Taylor & Francis. The accuracy of the Content should not be relied upon and should be independently verified with primary sources of information. Taylor and Francis shall not be liable for any losses, actions, claims, proceedings, demands, costs, expenses, damages, and other liabilities whatsoever or howsoever caused arising directly or indirectly in connection with, in relation to or arising out of the use of the Content.

This article may be used for research, teaching, and private study purposes. Any substantial or systematic reproduction, redistribution, reselling, loan, sub-licensing, systematic supply, or distribution in any form to anyone is expressly forbidden. Terms &

Journal of Coordination Chemistry
Vol. 66, No. 4, 20 February 2013, 612–623

Taylor & Francis
Taylor & Francis Group

Two copper(II) metal–organic networks derived from bis-pyridyl-bis-amide ligands and aromatic polycarboxylates: a 2-D layered structure and a 4-connected trinodal 3-D topology

HONGYAN LIN, PENG LIU, JUWEN ZHANG, XIULI WANG* and GUOCHENG LIU

Department of Chemistry, Liaoning Province Silicon Materials Engineering Technology Research Centre, Bohai University, Jinzhou, P.R. China

(*Received 13 July 2012; in final form 19 October 2012*)

Two metal–organic coordination polymers, $[Cu_3(4\text{-bpcb})_2(1,2,4\text{-btc})_2(H_2O)_2]$ (**1**) and $[Cu_3(3\text{-bpcb})_3(btec)_{1.5}]$ (**2**), have been synthesized from hydrothermal reaction of copper chloride with mixed ligands [4-bpcb = N,N′-bis(4-pyridinecarboxamide)-1,4-benzene, 3-bpcb = N,N′-bis(3-pyridinecarboxamide)-1,4-benzene, 1,2,4-H_3btc = 1,2,4-benzenetricarboxylic acid, and H_4btec = 1,2,4,5-benzenetetracarboxylic acid]. X-ray diffraction analysis reveals that **1** exhibits a 2-D layer structure and **2** possesses a three-dimensional (3-D) network. In **1** and **2**, Cu^{II} ions are connected by bridging 1,2,4-btc or btec to form 2-D polymeric layers. Cu-1,2,4-btc layer does not propagate into a 3-D coordination framework in **1** due to 4-bpcb showing monodentate coordination (via ligation of only one pyridyl nitrogen). In **2**, Cu-btec 2-D layers are further extended into a 3-D network with $(6^4.8^2)_3$ topology by 3-bpcb ligand in μ_2-bridging coordination (via ligation of two pyridyl nitrogens). The different structures of the two complexes illustrate the influence of different polycarboxylates and N-donor positions of organic ligands on the formation of such coordination architectures. Moreover, the thermal properties and electrochemical properties of the copper complexes bulk-modified carbon paste electrodes have been studied.

Keywords: Hydrothermal reaction; Polycarboxylate; Bis-pyridyl-bis-amide ligand; Crystal structure; Electrochemical property

1. Introduction

Design and construction of metal–organic coordination complexes is interesting due to their novel structural topologies and potential applications in catalysis, gas storage, molecular adsorption, and magnetic materials [1–4]. Self-assembly of these complexes can be realized by selection of organic ligands and metal ions [5–7]. Aromatic polycarboxylates to construct coordination complexes are of high interest [8–10]. Thus, 1,3,5-benzenetricarboxylic acid (1,3,5-H_3BTC) [11], 1,2,4-benzenetricarboxylic acid (1,2,4-H_3btc) [12], and 1,2,4,5-benzenetetracarboxylic acid (H_4btec) [13, 14] have proven efficacious towards preparation of metal–organic coordination complexes. Aromatic polycarboxylic acids and

---

*Corresponding author. Email: wangxiuli@bhu.edu.cn

Journal of Coordination Chemistry
ISSN 0095-8972 print/ISSN 1029-0389 online © 2013 Taylor & Francis
http://dx.doi.org/10.1080/00958972.2013.766333

analogs of dipyridyl-type ligands have been utilized to bridge metal ions, leading to complexes with fascinating structures and interesting properties [15–19].

Based on two types of bis(pyridylformyl)piperazine ligands and aromatic polycarboxylates, LaDuca *et al.* and our group have reported a series of 2-D and 3-D polymers, such as a 3,5-connected binodal 3-D polymer [Cu(3-bpfp)(1,3,5-HBTC)]$\cdot H_2O$ (3-bpfp = bis(3-pyridylformyl)piperazine) with $(4.5^3.8^2.9^4)_3(4.5^2)_2$ topology [20], a 4,4-connected binodal layer structure $[Cu_2(BDC)_2(4\text{-bpfp})(H_2O)_2]_n$ with $(4.6^48)_2(4^26^4)$ topology, and a 4,5-connected binodal 3-D network $[Cd_2(BDC)_2(4\text{-bpfp})(H_2O)_2]_n$ with rare $(4^46^2)(4^46^6)$ tcs topology (H_2BDC = 1,2-benzenedicarboxylic acid, 4-bpfp = bis(4-pyridylformyl)piperazine) [21, 22]. With bis-pyridyl-bis-amide N,N′-bis(4-pyridinecarboxamide)-1,4-benzene (4-bpcb) and 1,3,5-H_3BTC, we have obtained a 3-D metal–organic coordination polymer, $[Cu_3(4\text{-bpcb})_3(1,3,5\text{-BTC})_2]_3\cdot\sim 12H_2O$, wherein discrete $(H_2O)_{12}$ clusters are dispersed in the threefold interpenetrating 3-D metal–organic framework [23].

As an extension of our study on assembly of metal/dipyridyl-type ligands/carboxylate hybrid systems [19, 20, 23], two isomeric bis-pyridyl-bis-amide ligands 4-bpcb and N,N′-bis(3-pyridinecarboxamide)-1,4-benzene (3-bpcb) are selected as neutral N-donors to be introduced into metal–polycarboxylate systems with expectation to obtain high-dimensional structures. As a result, two Cu(II) coordination polymers, $[Cu_3(4\text{-bpcb})_2(1,2,4\text{-btc})_2(H_2O)_2]$ (**1**) and $[Cu_3(3\text{-bpcb})_3(btec)_{1.5}]$ (**2**), have been obtained. Complex **1** is a 2-D layer structure based on 1,2,4-btc and 4-bpcb, extended into a 3-D supramolecular structure by hydrogen-bonding interactions. Complex **2** exhibits a 3-D coordination polymeric network bridged by btec and 3-bpcb. Thermal properties and electrochemical behaviors of **1** and **2** are also reported.

2. Experimental

2.1. *Materials and methods*

4-Bpcb and 3-bpcb were synthesized by literature methods [24]; 1,2,4-btc and btec were commercially obtained and used without purification. All other reagents were of reagent grade. FT-IR spectra (KBr pellets) taken on a Magna FT-IR 560 Spectrometer and elemental analyses (C, H, and N) were carried out on a Perkin–Elmer 2400 CHN elemental analyzer. Thermogravimetric analyses were performed with a Pyris Diamond TG-DTA instrument. The electrochemical experiments were carried out with a CHI 440 Electrochemical Quartz Crystal Microbalance. A conventional three-electrode cell was used at room temperature. Complexes **1** and **2** bulk-modified carbon paste electrodes (**1**-CPE and **2**-CPE) were used as working electrodes. An SCE and a platinum wire were used as reference and auxiliary electrodes, respectively. The bulk-modified CPEs were fabricated by methods of the literature [23].

2.2. *Preparation of the complexes*

2.2.1. Synthesis of $[Cu_3(4\text{-bpcb})_2(1,2,4\text{-btc})_2(H_2O)_2]$ (1). Complex **1** was prepared by simple hydrothermal reaction of $CuCl_2\cdot 2H_2O$ (0.051 g, 0.3 mmol), 4-bpcb (0.040 g, 0.13 mmol), 1,2,4-H_3btc (0.025 g, 0.12 mmol), H_2O (12 mL), and NaOH (0.018 g, 0.45 mmol). The mixture was stirred for 30 min in air, then transferred and sealed in a

25 mL Teflon reactor, which was heated at 120 °C for four days, leading to the formation of blue block crystals of **1** (22% yield based on Cu). Anal. Calcd for $C_{54}H_{38}N_8O_{18}Cu_3$: C, 50.72; H, 3.00; N, 8.77%. Found: C, 50.75; H, 3.06; N, 8.72%. IR (KBr, cm^{-1}): 3512s, 3370m, 3296m, 3039w, 2680m, 2363m, 2335m, 2214w, 1645s, 1612s, 1551s, 1511s, 1402s, 1375s, 1321s, 1301w, 1267m, 1227s, 1132m, 1112w, 1064m, 1010m, 977w, 929m, 889m, 827s, 794m, 747m, 706m, 672s, 605 m, 571m, 530m.

2.2.2. Synthesis of [Cu_3(3-bpcb)$_3$(btec)$_{1.5}$] (2). A mixture of $CuCl_2 \cdot 2H_2O$ (0.051 g, 0.3 mmol), H_4btec (0.003 g, 0.12 mmol), 3-bpcb (0.060 g, 0.19 mmol), H_2O (12 mL), and NaOH (0.018 g, 0.45 mmol) was stirred for 30 min in air, then transferred and sealed in a 25 mL Teflon reactor, which was heated at 120 °C for four days, leading to the formation of blue block crystals of **2** (27% yield based on Cu). Anal. Calcd for $C_{23}H_{15}N_4O_6Cu$: C, 54.45; H, 2.98; N, 11.05%. Found: C, 54.40; H, 2.94; N, 11.09%. IR (KBr, cm^{-1}): 3316s, 3201s, 3113m, 3059w, 2775m, 2667m, 2599w, 2363m, 2322m, 2214w, 1639s, 1605s, 1551s, 1518m, 1396s, 1294s, 1234s, 1132m, 1058m, 1031m, 977w, 956w, 923m, 734m, 760s, 699m, 679s, 612m, 578s, 537s.

2.3. *X-ray crystallography*

Crystallographic data for the two complexes were collected on a Bruker Apex CCD diffractometer with Mo Kα ($\lambda = 0.71073$ Å for **1** and $\lambda = 0.71069$ Å for **2**) by ω scan mode. The structures were solved by direct methods using SHELXS of the SHELXTL package and refined by full-matrix least-squares methods with SHELXL [25, 26]. Coppers in the complexes were located from *E*-maps and all non-hydrogen atoms refined anisotropically. For **1**, hydrogens of coordinated water could not be located and were directly included in the

Table 1. Crystal data and structure refinements for **1** and **2**.

Formula	$C_{54}H_{38}Cu_3N_8O_{18}$	$C_{23}H_{15}CuN_4O_6$
Formula wt.	1277.54	506.93
Cryst. syst.	Monoclinic	Triclinic
Space group	P 21/c	P-1
a (Å)	13.9126(15)	9.047(5)
b (Å)	10.0812(11)	10.0812(11)
c (Å)	17.1931(18)	13.506(5)
α (°)	90	102.100(5)
β (°)	92.265(2)	99.975(5)
γ (°)	90	106.945(5)
V (Å^3)	2409.5(4)	1000.7(9)
Z	2	2
D_{calc} (g cm^{-3})	1.761	1.682
μ (mm^{-1})	1.405	1.145
F(0 0 0)	1298.0	516
θ_{max} (°)	25.00	24.99
R_{int}	0.0458	0.0211
$R_1{}^a$ [$I > 2\sigma(I)$]	0.0518	0.0529
$wR_2{}^b$ (all data)	0.1611	0.1921
GOF	1.062	1.059
$\Delta\rho_{max}$ (e Å^{-3})	0.914	1.282
$\Delta\rho_{min}$ (e Å^{-3})	−1.120	−1.227

$^aR_1 = \Sigma||F_o|-|F_c||/\Sigma|F_o|$; $^bwR_2 = \Sigma[w(F_o{}^2-F_c{}^2)^2]/\Sigma[w(F_o{}^2)^2]^{1/2}$.

final molecular formula. Hydrogens of 4-bpcb or 3-bpcb were generated theoretically onto specific atoms and refined isotropically with fixed thermal factors. A summary of crystal data and structure refinements for the two complexes is provided in table 1. Selected bond lengths and angles are listed in tables S1 and S2. Hydrogen-bonding geometries of **1** are given in table S3. CCDC 851403 for **1** and 851404 for **2** contain the supplementary crystallographic data for this paper. These data can be obtained free of charge from The Cambridge Crystallographic Data Center via www.ccdc.cam.ac.uk/data_request/cif.

3. Results and discussion

3.1. *Description of crystal structures for 1 and 2*

3.1.1. $[Cu_3(4\text{-bpcb})_2(1,2,4\text{-btc})_2(H_2O)_2]$ (1). Single crystal X-ray diffraction analysis reveals that **1** consists of three Cu^{II} ions, two 4-bpcb, two coordinated waters and two 1,2,4-btc bridging ligands. In **1**, there are two crystallographically independent Cu^{II} ions [Cu(1) and Cu(2)], as shown in figure 1. Cu(1) is four-coordinated by one nitrogen from 4-bpcb, two oxygens from two carboxyl groups of two different 1,2,4-btc ligands and one coordinated water. The bond distances and angles around Cu(1) ion are 1.955(3), 1.968(3), and 1.913(4) Å for Cu–O, 2.019(4) Å for Cu–N, 88.39(13)°–163.80(18)° for O–Cu–O, and 87.80(15)°–171.32(15)° for O–Cu–N. Cu(2) is also four-coordinated by three carboxyl oxygens from three 1,2,4-btc ligands, and one coordinated water. The coordination of Cu (2) is a slightly distorted quadrangle. The bond distances and angles around Cu(2) are 1.880(4) and 1.974(3) Å for Cu–O, and 88.84(16)°, 91.16(16)° and 180.0° for O–Cu–O angle, respectively. The O(4)–O(5W)–Cu(2)–O(4#1)–O(5W#1) five-membered unit is planar.

In **1**, 1,2,4-btc is monodentate-bis(monodentate) coordination (see chart 1(a)): one carboxyl is monodentate and coordinated with Cu(1) while another is simultaneously coordinated to Cu(1) and Cu(2) in a bis(monodentate) bridging mode; the third is not coordinated. Adjacent two Cu(1) and one Cu(2) ions are linked by carboxyl of 1,2,4-btc with bis(monodentate) bridging to form a trinuclear copper cluster, further connected by the carboxyl of 1,2,4-btc with monodentate and bis(monodentate) modes to construct a

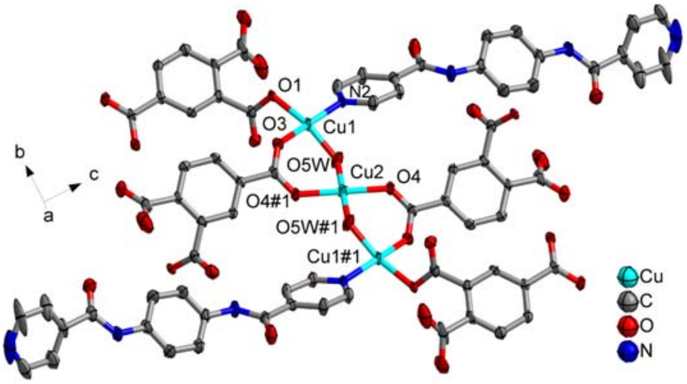

Figure 1. The coordination environment for Cu^{II} in **1** (at 50% probability). (All hydrogens and lattice waters are omitted for clarity.)

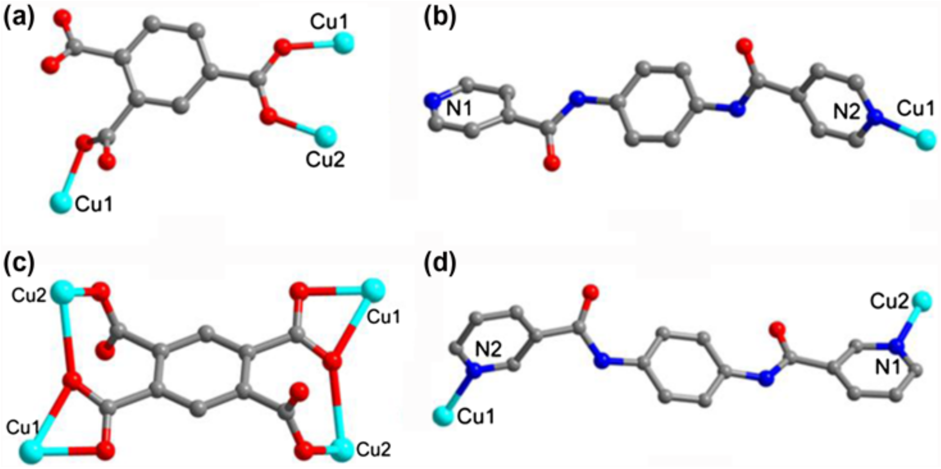

Chart 1. Coordination modes of 1,2,4-btc (a), 4-bpcb (b), btec (c), and 3-bpcb (d) in **1** and **2**.

2-D Cu-1,2,4-btc layer, as shown in figure 2(a) and figure S1a (Supporting Information). Each Cu^{II} [Cu(1), Cu(2)] is linked to four adjacent Cu^{II} ions by two 1,2,4-btc ligands, which can be regarded as 2-connected nodes. Each 1,2,4-btc is surrounded by three Cu^{II} ions, defined as a 3-connected node. So, the topology of the 2-D Cu-1,2,4-btc layer of **1** is $(12^3)_2(12)_3$, in which the dodecanuclear cycle is composed of six 1,2,4-btc ligands and six Cu^{II} ions [three Cu(1) and three Cu(2)] (figure 2(b)). 4-Bpcb shows monodentate coordination (chart 1(b)) with only one pyridyl nitrogen coordinated to Cu^{II}, and the corresponding dihedral angle between the pyridyl rings is 89.86°. These Cu-1,2,4-btc 2-D layers are not extended into a 3-D coordination framework in **1** due to monodentate 4-bpcb (figure S1b, Supporting Information). Hydrogen bonding between nitrogen of 4-bpcb and the carbonyl oxygen from 4-bpcb [N(3)–H(3A)···(O_8) = 3.087(6) å] results in a 3-D supramolecular framework for **1** (figure 3).

3.1.2. $[Cu_3(3\text{-bpcb})_3(btec)_{1.5}]$ (2). Complex **2** is a 3-D coordination polymer composed of a twisted 2-D Cu-btec layer and 3-bpcb. As illustrated in figure 4, each Cu(1) is six-coordinated distorted octahedral, ligated by two nitrogens from two different bidentate 3-bpcb ligands with bond distances of 1.999(4) Å [Cu(1)–N(2), Cu(1)–N(2)#1], and four oxygens of two carboxyl groups from two different btec [bond lengths of Cu(1)–O range from 2.057(4) to 2.337(4) å]. Cu(2) is also coordinated by two nitrogens from two 3-bpcb ligands with Cu(2)–N distance of 2.050(4) Å and N(1)–Cu(2)–N(1)#1 angle of 180.00(1)°, and four carboxyl oxygens from two btec with Cu(2)–O distances of 1.948(4)–2.471(4) Å, O(3)–Cu(2)–O(3)#1 or O(2)–Cu(2)–O(2)#1 angle is 180.00(1)°, showing distorted octahedral geometry. Cu(2) displays remarkable differences in Cu–O bond length, which may be attributed to the Jahn–Teller effect. In **2**, all carboxyl groups of btec are deprotonated and btec exhibits only one coordination mode (see chart 1(c)). The four carboxyl groups show deviations from the plane of the central aromatic ring due to rotation of the carboxyl groups, with arrangements above and below the plane. The four carboxyl groups show two different coordinations. Two carboxyl groups are monodentate with one oxygen bonding Cu, while the other two display chelating-monodentate linking two Cu ions. Hence, btec serves as a μ_4-bridge, linking four Cu centers through its four arms in two kinds of

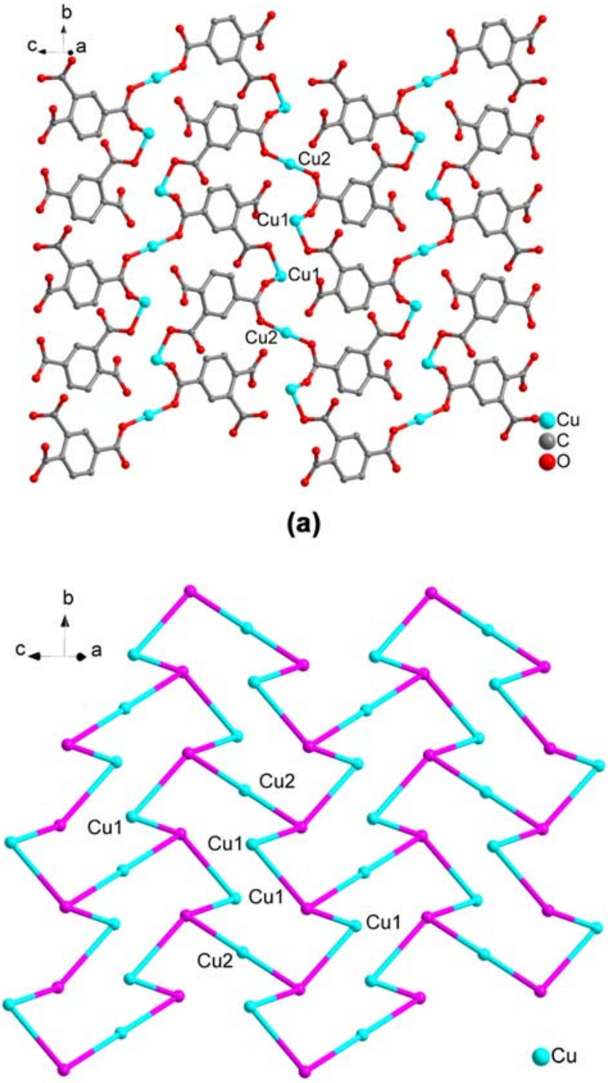

Figure 2. (a) The 2-D layer of **1** extended by bridging 1,2,4-btc. (b) The schematic of 2-D Cu-1,2,4-btc polymeric layer for **1**.

coordination to form an infinite 2-D Cu-btec polymeric layer, as shown in figure 5(a) (figure S2a, Supporting Information). In the 2-D Cu-btec layer, Cu^{II} [Cu(1) and Cu(2)] can be viewed as 2-connected nodes through two btec; the btec ligating with four Cu^{II} ions acts as a 4-connected ligand. Thus, a 2-D layer has been constructed, which can be clearly seen from figure 5(b). Different from **1**, there exists one octanuclear cycle composed of four btec ligands and four Cu^{II} ions [two Cu(1) and two Cu(2) ions] in the 2-D Cu-btec structure.

Cu(1) and Cu(2) belonging to adjacent 2-D Cu-btec polymeric layers are bridged by 3-bpcb to form a 3-D coordination network (figure 6(a) and figure S2c), in which 3-bpcb

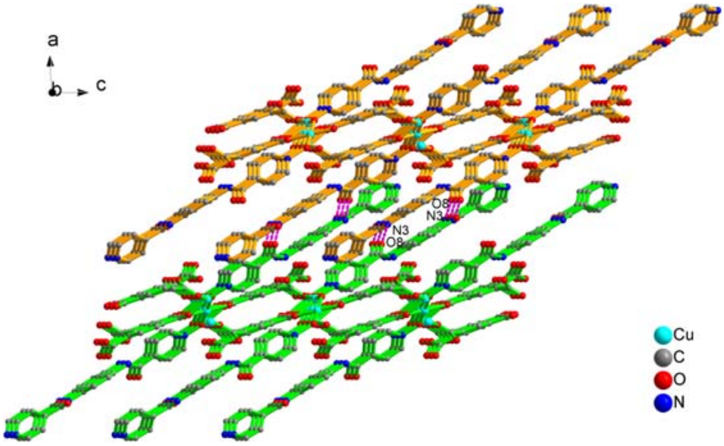

Figure 3. The 3-D supramolecular network of **1** formed by hydrogen-bonding interactions. (Hydrogens and lattice waters are omitted for clarity.)

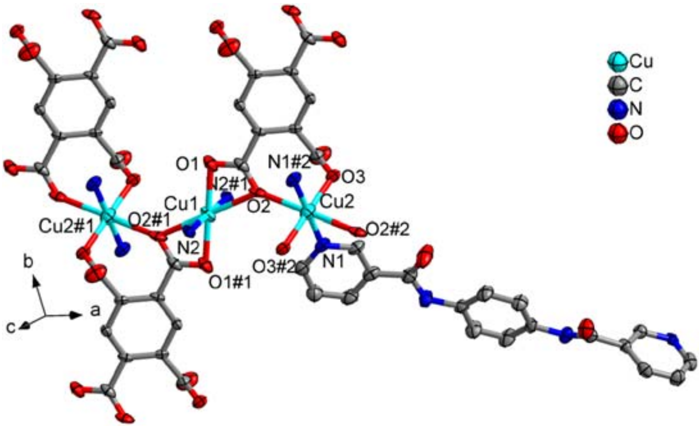

Figure 4. The coordination environment for Cu^{II} in **2** (at 50% probability). (All hydrogens, partial 3-bpcb, and btec are omitted for clarity.)

connect adjacent Cu^{II} ions with Cu(1)···Cu(2) distance of 16.69 Å (figure S2b, Supporting Information). Different from the coordination of 4-bpcb in **1**, which is only monodentate to one Cu^{II}, 3-bpcb is μ_2-bridging in the 3-D network of **2** (see chart 1(d)), similar to previous reports [19, 23]; the corresponding dihedral angle between pyridyl rings is 88.50°. In the 3-D network of **2**, both Cu(1) and Cu(2) are surrounded by four ligands (two bridging 3-bpcb and two bridging btec) and can be regarded as 4-connected nodes. Each btec is further linked to four copper ions [two Cu(1) and two Cu(2) ions], therefore, also defined as a 4-connected node, and 3-bpcb ligating with two 4-connected copper ions [Cu(1) and Cu(2)] only serves as a linear linker. Upon considering the Cu(1), Cu(2) ions, and btec ligands as nodes, the 3-bpcb ligands as spacers, the 3-D network of **2** can be described as a unique trinodal 4-connected network, as shown in figure 6(b). Its Schläfli symbol is $(6^4.8^2)_3$.

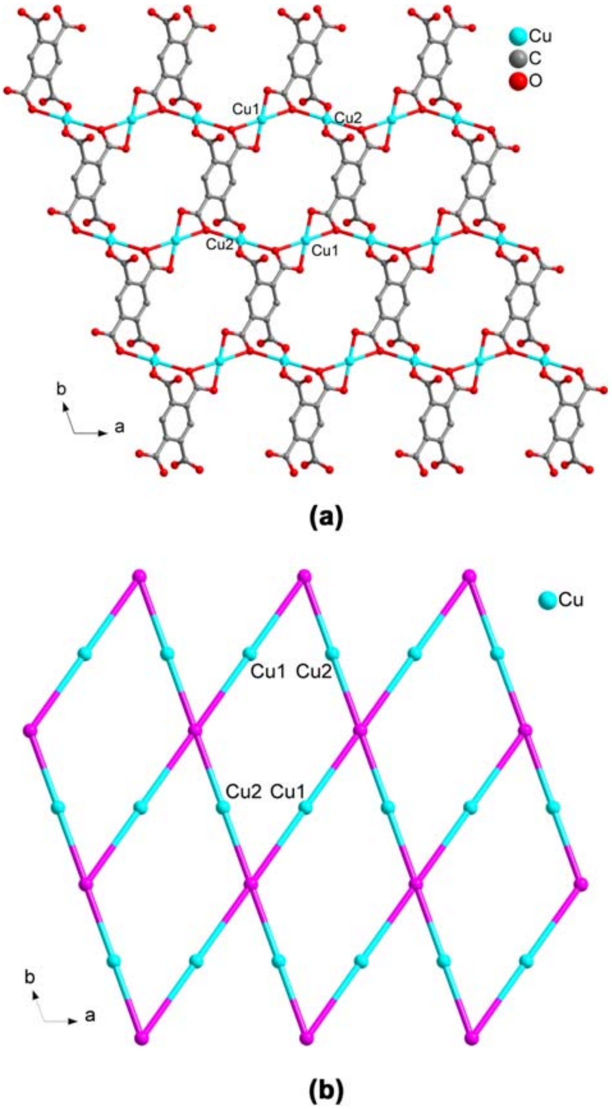

Figure 5. (a) The 2-D layer of 2 formed by bridging btec along the c-axis. (b) The schematic of 2-D Cu-btec polymeric layer for 2.

Many factors affect the crystallization and structural construction of complexes formed under hydrothermal conditions, such as initial reactants, reactant ratio, temperature, and pH. In our previous report, we obtained $[Cu_3(4\text{-bpcb})_3(1,3,5\text{-BTC})_2]_3 \cdot \sim 12H_2O$ employing 1,3,5-H_3BTC and 4-bpcb as ligands, in which discrete $(H_2O)_{12}$ clusters are dispersed in the threefold interpenetrating 3-D metal–organic framework [23]. To investigate the effect of different factors on assembly of metal–organic complexes, we attempted to synthesize different complexes by choosing different polycarboxylates, adjusting the reactants ratio and pH. Under similar conditions to a previous report [23], we expected that using 1,2,4-btc in place of 1,3,5-BTC would lead to a complex, yet, we were unable to obtain a crystalline complex. Only when the reactant ratio (Cu : 1,2,4-btc:4-bpcb) was changed to

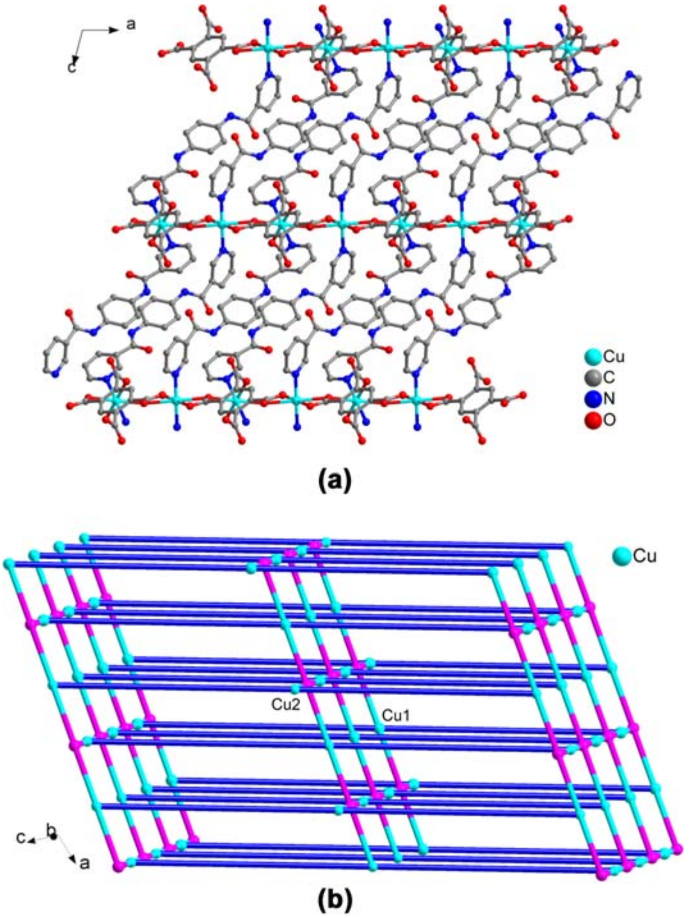

Figure 6. (a) The 3-D framework in **2** constructed by 3-bpcb and btec along the b-axis. (b) The schematic of the 3-D polymeric framework in **2**.

3 : 1.2 : 1.3 (in reference 23, the ratio of Cu : 1,3,5-BTC:4-bpcb is 2 : 1.2 : 1), the 2-D complex **1** with a $(12^3)_2(12)_3$ topology was successfully isolated, which is different from that of $[Cu_3(4\text{-bpcb})_3(1,3,5\text{-BTC})_2]_3 \cdot \sim 12H_2O$ [23]. To further study the structural diversity that can be tuned by different N-donors, we extended our studies from 4-bpcb to 3-bpcb. However, in the system composed of 3-bpcb and 1,3,5-BTC/1,2,4-btc, by means of adjusting the reactant ratio and systematic pH, no crystalline product was obtained. Thus, we introduced H_4btec into the Cu-4-bpcb/Cu-3-bpcb system. Although we adjusted the reactants ratio and systematic pH, only **2** based on 3-bpcb was obtained, which may be because syntheses of the complexes are affected not only by the stoichiometries of the reactants but also by the types of co-ligands in the reaction medium [27, 28].

In **1** and **2** based on two isomeric bis-pyridyl-bis-amide ligands (4-bpcb and 3-bpcb) and different polycarboxylates (1,2,4-btc or btec), coordination modes of polycarboxylates and bis-pyridyl-bis-amide ligands are different. In **1**, Cu^{II} ions are linked by 1,2,4-btc to generate a 2-D Cu-1,2,4-btc layer, in which the two carboxyl groups of 1,2,4-btc display monodentate-bis(monodentate) coordination and the third one is not coordinated with Cu^{II};

all carboxyl groups of btec are coordinated to Cu^{II} in **2**, two monodentate, and the other two chelating-monodentate. Thus, the 2-D Cu-btec layer of **2** is constructed. In **1** and **2**, 4-bpcb and 3-bpcb exhibit two different coordination modes, monodentate for 4-bpcb and μ_2-bridging for 3-bpcb. In **1**, monodentate 4-bpcb is coordinated to one Cu^{II}, resulting in a 2-D Cu-1,2,4-btc layer with 3-connected $(12^3)_2(12)_3$ topology, but not a 3-D framework. In **2**, the μ_2-bridging 3-bpcb ligands connect Cu^{II} ions to build a 1-D Cu–3-bpcb chain with Cu···Cu distance of 16.69 Å, ultimately resulting in a 3-D coordination network with trinodal 4-connected $(6^4.8^2)_3$ topology. The diversities of the final structures for **1** and **2** can be mainly ascribed to the different coordination of the isomeric bis-pyridyl-bis-amide ligands; the polycarboxylates (1,2,4-btc or btec) also show some effect.

3.2. *Thermal gravimetric analysis*

The thermal gravimetric (TG) analyses of **1** and **2** were determined from 30 to 600 °C (figure S3). For **1**, the first weight-loss step beginning at 165 °C is attributed to loss of coordinated water (3.11%, Calcd 2.82%). The second weight loss is observed from 280 to 520 °C, demonstrating loss of 1,2,4-btc and 4-bpcb. The TG curve of **2** shows only one obvious weight loss at 310 °C, assigned to decomposition of **2** and attributed to loss of btec and 3-bpcb. The weight loss of 83.82% is in agreement with calculated value of 84.22%. The remaining weight (18.44% for **1**, 16.18% for **2**) corresponds (18.79% for **1**, 15.78% for **2**) to Cu and O components, indicating that the final product is CuO.

3.3. *Electrochemical behaviors of the 1-CPE and 2-CPE*

For copper complexes, the ability to undergo reversible one-electron redox process is attractive for electrochemistry [29, 30]. **1** and **2** are hydrothermally synthesized and insoluble in water and common organic solvents. Thus, **1** and **2** bulk-modified carbon paste electrodes (**1**-CPE and **2**-CPE) are optimal to study their electrochemistry. Electrochemical studies of **1**-CPE and **2**-CPE are carried out in 0.1 M H_2SO_4 aqueous solution at

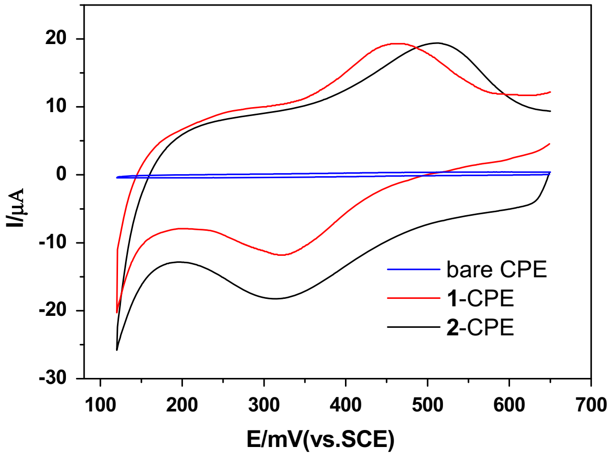

Figure 7. Cyclic voltammograms of bare CPE, **1**- and **2**-modified CPEs (**1**-CPE and **2**-CPE) in 0.1 M H_2SO_4 aqueous solution from 650 to 120 mV. Scan rate: 60 mV s^{-1}.

60 mV s^{-1}. In the potential range from 650 to 120 mV (figure 7), there is no redox peak at bare CPE. While for **1**-CPE and **2**-CPE, reversible redox peaks attributed to Cu^{II}/Cu^{I} are observed [19], the mean peak potentials $E_{1/2} = (E_{pa} + E_{pc})/2$ are +390 mV for **1**-CPE and +410 mV for **2**-CPE.

The effect of scan rates on the electrochemical behavior of the **1**-CPE and **2**-CPE was investigated from 650 to 120 mV in 0.1 M H_2SO_4 aqueous solution (figure S4 and figure S5). When the scan rates were varied from 20 to 250 mV s^{-1} for **1**-CPE (or 20–350 mV s^{-1} for **2**-CPE), the peak potentials change gradually: the cathodic peak potentials shift negative and the corresponding anodic peak potentials shift positive with increasing scan rates. Plots of peak currents *vs.* scan rates were shown in insets of figure S4 and figure S5. The anodic and cathodic currents were proportional to the scan rates, suggesting that redox processes for **1**-CPE and **2**-CPE were surface-confined.

4. Conclusion

We have synthesized two copper(II) complexes with aromatic polycarboxylates and isomeric bis-pyridyl-bis-amide ligands, $[Cu_3(4\text{-bpcb})_2(1,2,4\text{-btc})_2(H_2O)_2]$ (**1**) and $[Cu_3(3\text{-bpcb})_3(btec)_{1.5}]$ (**2**). Complex **1** exhibits a 3-D supramolecular structure, while **2** possesses a 3-D coordination polymeric network. The different structures of the two complexes illustrate the influence of different polycarboxylates and N-donor positions of ligands. **1** and **2** were employed to fabricate bulk-modified CPEs due to their insolubility. Preliminary results of **1**-CPE and **2**-CPE indicate potential candidates for electrochemical materials.

Acknowledgments

This work was supported by New Century Excellent Talents in University (NCET-09-0853), the National Natural Science Foundation of China (21171025 and 21101015), and the Natural Science Foundation of Liaoning Province (No. 201102003).

References

[1] O.M. Yaghi, M. Okeeffe, N.W. Ockwig, H.K. Chae, M. Eddaoudi, J. Kim. *Nature*, **423**, 705 (2003).
[2] X.L. Wang, C. Qin, E.B. Wang, Z.M. Su. *Chem. Eur. J.*, **12**, 2680 (2006).
[3] Y.N. Chi, K. Huang, S.W. Zhang, F.Y. Cui, C.W. Hu. *Cryst. Growth Des.*, **7**, 2449 (2007).
[4] F. Blank, C. Janiak. *Coord. Chem. Rev.*, **253**, 827 (2009).
[5] X.Q. Liang, X.H. Zhou, C. Chen, H.P. Xiao, Y.Z. Li, J.L. Zuo, X.Z. You. *Cryst. Growth Des.*, **9**, 1041 (2009).
[6] W.L. Zhang, Y.Y. Liu, J.F. Ma. *Cryst. Growth Des.*, **8**, 1250 (2008).
[7] Q.G. Zhai, C.Z. Lu, X.Y. Wu, S.R. Batten. *Cryst. Growth Des.*, **7**, 2332 (2007).
[8] Z.H. Zhang, S.C. Chen, J.L. Mi, M.Y. He, Q. Chen, M. Du. *Inorg. Chem.*, **46**, 8427 (2010).
[9] M.D. Stephenson, M.J. Hardie. *Cryst. Growth Des.*, **6**, 423 (2006).
[10] Z.Q. Liu, Y.T. Li, Z.Y. Wu, S.F. Zhang. *Inorg. Chim. Acta*, **362**, 71 (2009).
[11] K. Davies, S.A. Bourne, L. Öhström, C.L. Oliver. *Dalton Trans.*, 2869 (2010).
[12] P. Mahata, M. Prabu, S. Natarajan. *Inorg. Chem.*, **47**, 8451 (2008).
[13] C. Ren, L. Hou, B. Liu, G.P. Yang, Y.Y. Wang, Q.Z. Shi. *Dalton Trans.*, 793 (2011).
[14] H.Y. Lin, H.L. Hu, X.L. Wang, B. Mu, J. Li. *J. Coord. Chem.*, **62**, 1295 (2010).
[15] Y. Gong, J. Li, J.B. Qin, T. Wu, R. Cao, J.H. Li. *Cryst. Growth Des.*, **11**, 1662 (2011).
[16] L.F. Ma, Q.L. Meng, C.P. Li, B. Li, L.Y. Wang, M. Du, F.P. Liang. *Cryst. Growth Des.*, **10**, 3063 (2010).
[17] H.L. Jiang, Y. Tatsu, Z.H. Lu, Q. Xu. *J. Am. Chem. Soc.*, **132**, 5586 (2010).
[18] C.Y. Wang, Z.M. Wilseck, R.M. Supkowski, R.L. LaDuca. *Cryst Eng Comm*, **13**, 1391 (2011).

[19] X.L. Wang, B. Mu, H.Y. Lin, G.C. Liu. *J. Organomet. Chem.*, **696**, 2313 (2011).

[20] X.L. Wang, H.Y. Lin, B. Mu, A.X. Tian, G.C. Liu, N.H. Hu. *CrystEngComm*, **13**, 1990 (2011).

[21] Z.M. Wilseck, C.M. Gandolfo, R.L. LaDuca. *Inorg. Chim. Acta*, **363**, 3865 (2010).

[22] J.S. Lucas, A.L. Pochodylo, R.L. LaDuca. *CrystEngComm*, **12**, 3310 (2010).

[23] X.L. Wang, H.Y. Lin, B. Mu, A.X. Tian, G.C. Liu. *Dalton Trans.*, 6187 (2010).

[24] M. Sarkar, K. Biradha. *Cryst. Growth Des.*, **6**, 202 (2006).

[25] G.M. Sheldrick. *SHELXS-97, Program for X-ray Crystal Structure Solution*, Göttingen University, Göttingen (1997).

[26] G.M. Sheldrick. *SHELXL-97, Program for X-ray Crystal Structure Refinement*, Göttingen University, Göttingen (1997).

[27] T.V. Mitkina, N.F. Zakharchuk, D.Y. Naumov, O.A. Gerasko, D. Fenske, V.P. Fedin. *Inorg. Chem.*, **47**, 6748 (2008).

[28] C.D. Zhang, S.X. Liu, B. Gao, C.Y. Sun, L.H. Xie, M. Yu, J. Peng. *Polyhedron*, **26**, 1514 (2007).

[29] V.T. Kasumov, A. Bulut, F. Köksal, M. Aslanoğlu, İ. Uçar, C. Kazak. *Polyhedron*, **25**, 1133 (2006).

[30] R. Balamurugan, M. Palaniandavar, M.A. Halcrow. *Polyhedron*, **25**, 1077 (2006).